Looking at the Li content in solution of the 10 samples (no. 74 to 83 in Table II–2–4), hot spring waters from Acupan Mine show the highest values, around 5 ppm, followed by the high Li content (1.4 to 2.0 ppm) of Itogon hot spring, with the other hot springs of Laboy, Dalupirip, Asin, Klondyke and Pugo having Li content of 0.1 ppm or less. Striking differences between hot waters of various origins were obtained.

The B concentrations are low (0.1 and 0.3 ppm) at Laboy and Dalupirip, high (a few ppm) at Itogon, Asin, Klondyke and Pugo and strikingly high (40 ppm) at Acupan Mine.

Low values of the B/Cl ratios were obtained at Pugo (0.01), Klondyke (0.03), Asin (0.04) and Laboy (0.05) and relatively high values were obtained at Acupan Mine (0.10 to 0.11), Dalupirip (0.14) and Itogon (0.27 to 0.30). These high ratio show that the reservoir of geothermal fluid at Acupan Mine, Dalupirip and Itogon are andesitic and/or mudy.

2–3–3 Geothermometric estimations deduced from geochemical characteristics of hot spring waters

Underground temperature deduced from the silica concentrations and alkali ratios of hot spring waters are shown on Table II–2–5. The temperature may be calculated from the silica concentration assuming either a process of heat conduction cooling (T_{sio_2} cond) or a process of adiabatic cooling (T_{sio_2} adia). The alkali temperature is calculated from the relative concentrations of Na, K and Ca, which is then further corrected for Mg content. These results are plotted on the diagram of Fig. II–2–27, where the arrows point from the Na–K–Ca calculated temperature to the Mg-corrected temperatures.

The spring water of Acupan Mine may be divided into two groups. One group (no. 15 to 17, 27 to 31, 35 to 37, 48, 50, 52, 65, 72, 82, 83) shows very high underground temperatures, i.e. T_{sio_2} ranging from 147 to 229°C and $T_{Na-K-Ca}$ between 193 and 236°C, before Mg-correction. The other group (no. 32 to 34, 38 to 41, 66, 67) shows low temperatures, with T_{sio_2} less than 100°C and $T_{Na-K-Ca}$ less than 50°C. Furthermore, all samples of this group gave $T_{Na-K-Ca} = 0$ after Mg correction, probably because these waters were formed by mixing with surface waters. These two groups also show marked contrast on their chemical composition. The high temperature spring water contains Cl^- as anion and $Na^+ + K^+$ as cations, while the low temperature group contains SO_4^{2-} as anion and Ca^{2+} as cation (Fig. II–2–23).

In the case of the Itogon hot spring water, T_{sio_2} ranges from 155 to 209°C. These high temperature waters compare well with that of the high temperature type of Acupan Mine.

For Antamok, two types of water may be distinguished on the basis of their silica concentration and alkali ratio temperature. One type (no. 18 to 20, 26, 70, 71) has T_{sio_2} ranging from 76 to 127°C and extreme low $T_{Na-K-Ca}$, and the other type (no. 69) with T_{sio_2} = 158°C and $T_{Na-K-Ca}$ = 169°C (and not zero after Mg correction). This distinction is also evident from the chemical composition of the waters, with the first type containing sulfate SO_4^{2-} and calcium Ca^{2+} as dominant ions and the second type containing chloride Cl^- and sodium $Na^+ + K^+$.

Waters from Laboy give high silica temperatures of 178 to 185°C and very low $T_{Na-K-Ca}$ of 6 to 20°C. Geochemically, they are similar to the low temperature type water of Acupan Mine and Antamok, differing only by their high T_{sio_2}.

Dalupirip water have low T_{sio_2} (91 to 102°C) and $T_{Na-K-Ca}$ (54 to 57°C) but their chemical composition resembles that of Itogon hot spring waters.

In the waters of Asin, Klondyke and Pugo, the anions and cations are Cl^- and $Na^+ + K^+$, respectively. They are geochemically similar to the high temperature waters of Acupan Mine, except that the geochemical temperature are low (T_{sio_2} = 46 to 144°C and $T_{Na-K-Ca}$ = 27 to 68°C).

The comparison between T_{sio_2} and $T_{Na-K-Ca}$ (Fig.II–2–27)shows that $T_{Na-K-Ca} > T_{sio_2}$ for the samples from Acupan Mine, Itogon and from the high temperature type of Antamok. As shown on Table II–2–5, these samples are also characterized by intermediate or slightly alkaline pH. Both characteristics suggest contamination of these waters by surface or ground waters, because such contamination lowers the silica concentration used in the calculation. On the other hand, the hot spring water samples of low temperature type from both Acupan Mine and Antamok, and the Laboy spring waters show $T_{sio_2} > T_{Na-K-Ca}$ in spite of their intermediate or alkaline character. This could mean that they are not in chemical equilibrium with the surrounding rocks. However, the silica concentration of the Laboy samples is extremely high; the reason for this is not clear.

2–3–4 Results of Isotopic Analysis of Hot Spring Waters

Oxygen and hydrogen isotopic ratios were measured in twelve samples: ten of them were from hot spring waters, one was taken from a small creak, east of Dalupirip and one is precipitate collected at the camp near Baguio City. The results are shown on Table II–2–6 together with those obtained by F.J. Sawkins et al. (1979).

Fig. II–2–28 was obtained from Table II–2–6. The line $\delta D = 8 \cdot \delta^{18}O + 10$ represents the "meteoric water line" after Craig (1963). The stream water sample from Dalupirip (DA) and that of precipitate (PRE) were plotted near this straight line. The samples from Pugo, Asin, Klondyke,

Table II–2–5 Table of T_{sio_2} & $T_{Na-k-ca}$ for Spring Water Samples (I) (1)

	Sample No.	pH	Temp	T_{SiO_2}		$T_{Na-K-Ca}$	T Mg
				adia	cond		
1	E 1	7.43	50.5	193	209	208	148
2	3	7.64	27.0	103	101	50	0
3	4	7.10	44.0	104	102	57	0
4	5	7.08	41.0	101	99	57	0
5	6	6.78	43.0	104	102	54	0
6	7	7.60	22.0	83	78	74	0
7	8	7.50	21.0	72	66	14	0
8	9	7.93	23.5	106	104	65	0
9	10	7.43	39.0	94	91	33	0
10	11	7.78	45.0	95	91	31	0
11	12	7.48	24.0	84	80	23	0
12	13	7.62	21.0	75	70	−12	0
13	14	7.76	23.0	99	97	18	0
14	15	7.28	19.0	70	63	−2	0
15	16	7.99	62.0	149	155	226	185
16	17	7.95	85.0	171	182	233	156
17	18	6.88	80.0	164	173	238	231
18	19	7.07	19.0	81	76	−15	0
19	20	6.20	20.0	92	89	−1	0
20	21	6.78	18.0	99	97	7	0
21	22	6.62	18.5	92	88	2	0
22	23	6.73	19.0	95	92	3	0
23	24	5.51	19.0	89	85	−5	0
24	25	5.30	18.0	94	91	−3	0
25	26	6.79	17.5	73	67	−8	0
26	Antamok	3.35	37.0	102	100	66	0
27	Benguet— 1	7.84	79.5	163	172	212	189
28	2	8.36	99.0	192	208	218	0
29	3	0.00	80.0	179	191	230	224
30	4	8.12	72.5	171	182	223	215
31	5	8.05	64.5	159	168	209	187
32	6	7.80	55.0	79	74	8	0
33	7	7.25	73.0	82	77	13	0
34	8	7.25	57.0	79	74	1	0
35	9	8.23	65.0	150	157	223	216
36	10	7.89	52.0	155	162	214	176
37	11	0.00	97.0	163	172	215	0
38	12	7.57	63.0	100	98	33	0
39	13	7.04	51.5	91	87	−6	0
40	14	7.61	0.0	89	85	−2	0
41	15	7.75	45.0	87	82	0	0
42	16	0.00	24.0	84	80	−7	0
43	17	0.00	43.0	87	82	49	0
44	18	7.47	94.0	149	155	210	186
45	19	7.37	85.0	135	139	201	129
46	20	8.78	70.0	87	82	68	0
47	21	7.43	41.0	87	82	27	0

Table II–2–5 Table of T_{sio_2} & $T_{Na-k-ca}$ for Spring Water Samples (2)

	Sample No.	pH	Temp	T_{SiO_2}		$T_{Na-K-Ca}$	T Mg
				adia	cond		
48	BED – 1	8.50	96.0	186	200	246	230
49	2	6.80	87.0	0	0	0	0
50	3	8.80	61.0	172	183	193	170
51	4	7.80	59.0	142	147	73	0
52	5	7.70	79.0	180	194	204	158
53	6	6.30	86.0	161	170	205	99
54	7	6.00	75.0	168	178	216	134
55	8	2.70	20.0	124	126	–10	0
56	9	3.90	20.0	120	121	17	0
57	10	4.20	19.5	110	110	–0	0
58	11	7.30	20.0	77	71	–25	0
59	12	8.20	20.0	81	76	–14	0
60	13	8.00	20.0	97	94	–14	0
61	14	8.00	20.0	103	102	–18	0
62	15	7.40	20.0	100	98	–31	0
63	16	7.40	20.0	75	69	–21	0
64	17	7.20	20.0	81	76	–13	0
65	76–B– 3	0.00	63.7	206	226	243	236
66	4	0.00	46.1	96	93	4	0
67	5	0.00	46.1	97	94	6	0
68	11	0.00	87.9	167	177	112	32
69	12	0.00	51.7	151	158	169	88
70	14	0.00	40.6	125	127	16	0
71	15	0.00	46.1	117	118	9	0
72	26	0.00	61.1	183	196	210	121
73	27	0.00	0.0	77	72	7	0
74	DA	7.90	42.5	94	91	55	0
75	IT – 1	7.68	89.5	163	172	203	115
76	2	7.79	62.2	154	161	202	130
77	KL	8.36	49.5	128	130	38	0
78	AS	8.64	73.8	140	144	68	0
79	PU	7.93	36.3	54	46	29	0
80	LA– 1	8.02	47.5	173	185	20	0
81	2	8.40	47.5	167	178	6	0
82	BA– 1	8.10	81.0	209	229	228	182
83	2	8.21	62.1	207	226	220	202

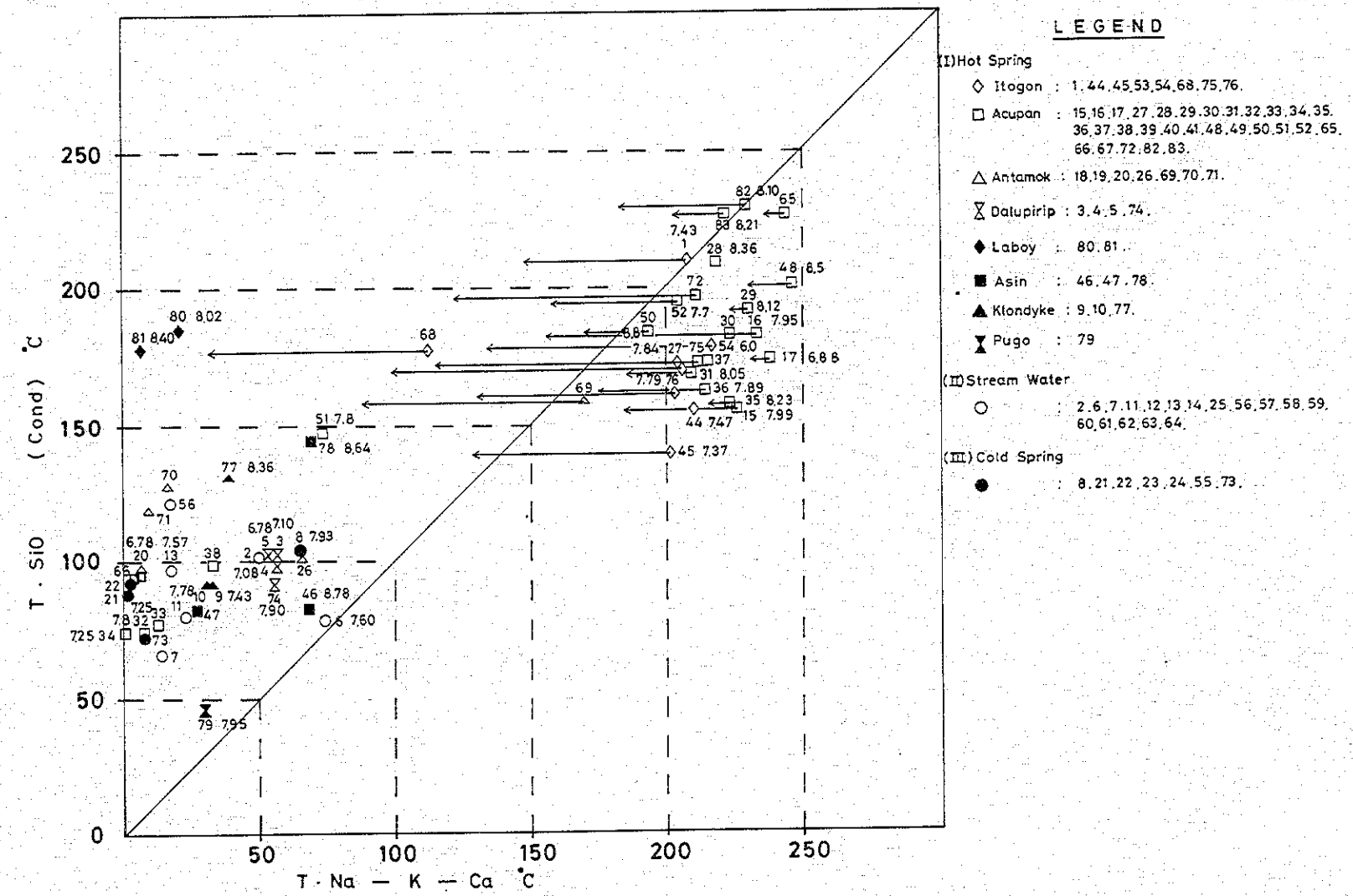

Fig. II–2–27 Diagram of Correlation of T_{SiO_2} with $T_{Na-K-Ca}$

Table II–2–6 Stable Isotope Analyses of Modern Thermal Waters and Stream Water Samples

Sample No.	Sample location	δD	$\delta^{18}O$	Reference
DA	Dalupirip, hot spring	–67.1	–9.8	BED–J1CA (1982)
IT–1	Itogon, hot spring	–67.2	–9.8	"
IT–2	Itogon, hot spring	–67.6	–9.6	"
KL	Klondykes, hot spring	–64.9	–9.2	"
AS	Asin, hot spring	–59.9	–8.5	"
PU	Pugo, hot spring	–55.4	–8.1	"
LA–1	Laboy, hot spring	–69.2	–10.1	"
LA–2	Laboy, hot spring	–70.7	–10.5	"
BA–1	Acupan mine, 3300^{L}, hot spring	–62.3	–7.7	"
BA–2	Acupan mine, 3150^{L}, hot spring	–62.5	–7.6	"
DA–ST	East of Dalupirip, stream	–71.0	–10.1	"
PRE	Precipitate at Baguio city	–66.9	–9.9	"
76–B–1		–65	–8.12	Sawkins F.J. et al. (1979)
76–B–3	Acupan mine, 3150^{L}, hot spring	–57	–6.54	"
76–B–4	Acupan mine, 2600^{L}, hot spring	–71	–10.71	"
76–B–5	Acupan mine, 2600^{L}, hot spring	–71	–10.45	"
76–B–11	Itogon, hot spring	–67	–2.17	"
76–B–12	Antamok mine, 1850^{L}, hot spring	–61	–5.82	"
76–B–14	Antamok mine, 1850^{L}, hot spring	–58	–10.23	"
76–B–15	Antamok mine, 1550^{L}, hot spring	–66	–9.30	"
76–B–26	Acupan mine, 3150^{L}, hot spring	–68	–8.12	"
76–B–27	Acupan mine, 1500^{L}, cold spring	–75	–11.48	"

Itogon and Laboy hot springs were also plotted near this meteoric water line. Samples from Acupan (76–B–4= 66, 76–B–5 = 67) and Antamok (76–B–15 = 71) analyzed by Sawkins et al. (1979) were likewise plotted near this line. The chemical compositions of these samples, on the other hand, (Fig. II–2–23, 24), show that except for the saline solutions from Asin, Klondyke and Pugo, SO_4^{2-} is the dominant anion in Acupan, Laboy and Dalupirip samples while Ca^{2+} is the dominant cation in Acupan and Laboy samples. Moreover, the geochemical temperatures (Fig. II–2–27) estimated from these samples are all very low.

The samples that plot away from Craig's meteoric water line are hot spring samples from Acupan (76–B–3 = 65, 76–B–26=72, BA–1=82, BA–2=83), Itogon (76–B–11=68) and Antamok (76–B–12=69). As shown by the key-diagrams (Fig. II–2–23, 24), Acupan, Itogon and Antamok waters have Cl^- and $Na^+ + K^+$ as major anions and cations. The estimated geochemical temperatures are the following: T_{sio_2} ranges from 158 to 229°C, $T_{Na-K-Ca}$ from 112 to 243°C (Table II–2–5). Samples from Acupan (76–B–3=65, 76–B–26=72, BA–1=82, BA–2=83), Itogon (76–B–11=68) and Antamok (76–B–12=69) show a shift of oxygen ($\delta^{18}O$).

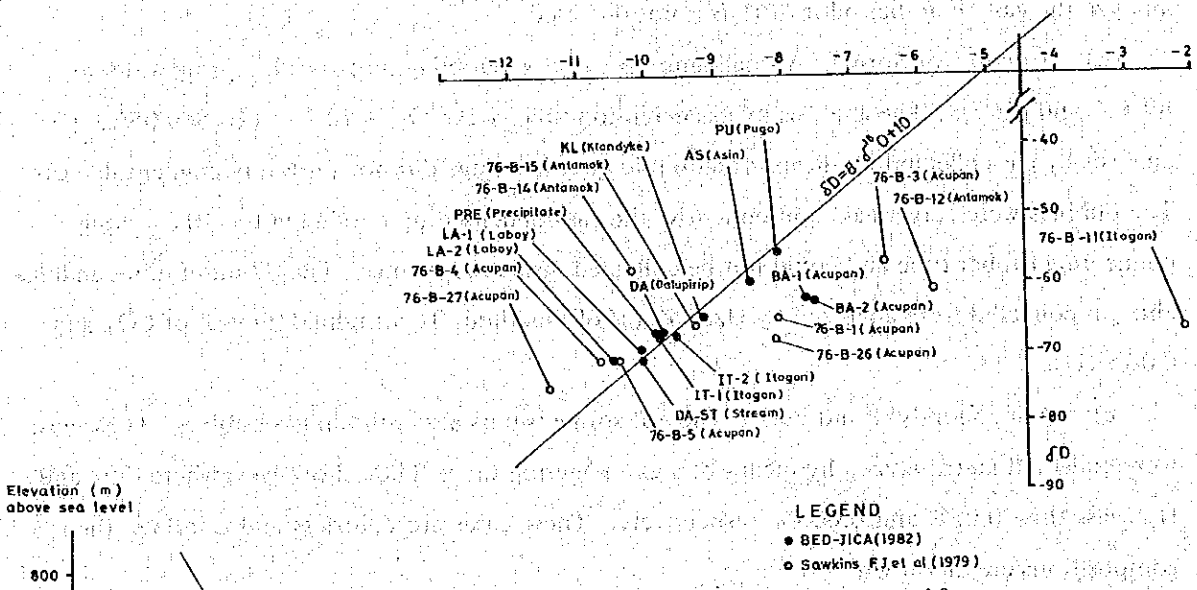

Fig. II–2–28 Plot of $\delta^{18}O$ for Water Samples

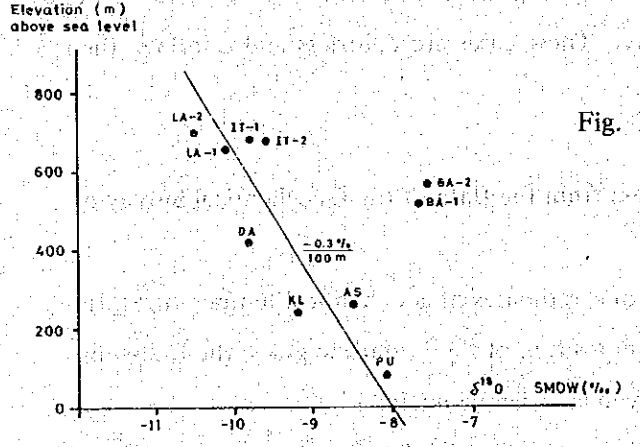

Fig. II–2–29 $\delta^{18}O$ Versus Elevation of Sampling Points

Fig. II–2–29 shows the relationship between the elevation a.s.l. of the sampling location and the $\delta^{18}O$ value. In order to estimate the coherence of the analytical precision, only the 10 samples of hot spring sampled in this survey are plotted on this diagram. It appears clearly that when the elevation increases by 100m, the $\delta^{18}O$ value decreases by 0.3‰ Samples from Laboy, Itogon, Dalupirip, Klondyke, Asin and Pugo lie along the meteoric line because these hot waters originate from local and very shallow ground water systems. The two samples from Acupan Mine (BA–1=82, BA–2=83) plot far from this line, which shows dilution of geothermal water.

2–3–5 Analysis of Fumerolic Gases

The main characteristics of the fumarolic gases and hot spring gases observed during these survey may be summarized as follows (Table II–2–3):

a) Acupan Mine, 3,150 level: Fumarolic gas, together with a large amount of water, are emitted from a drilling hole, but due to problems of security, it was impossible to collect and analyze the gas. Familiar odor of H_2S is not detected.

b) Itogon Hot Spring: A small amount of gas is bubbling up from the spring water at 89.5°C and pH 7.5. The analysis by gas detection tube gives $CO_2 > 20\%$ and H_2S=0.05%. The analysis by gas collected by means of a double mouth syringe did not show any condensable gas. The bubbles were very weak; consequently, the gas condensed by cooling in the 10 cm. long connecting rubber tube and could not be collected inside the syringe. The 87 ml of non-condensable gas collected were analyzed by Ozawa's (1969) method. It contained 99.94% of CO_2 and 0.06% H_2S.

c) Asin, Klondyke and Pugo: The hot spring waters also contain gas bubbles. These gases were collected and analyzed by means of a gas detection tube. They show everywhere CO_2 and H_2S less than 0.05% and 0.005%, respectively. These gases are colorless and odorless; their compositions are unknown.

2–3–6 Estimation of the Geothermal System from the Data of the Geochemical Survey of Hot Spring Waters.

Based on the data on chemical compositions, estimates of geochemical temperatures, isotopic composition of hot spring waters and composition of the fumarolic gases, the following considerations concerning system of the surveyed area can be made:

Among the samples from Acupan Mine, the water springing from within or around Balatoc plug (no. 15 to 17, 27 to 31, 35 to 37, 48, 50 to 52, 65, 72, 82, 83) are geochemically of the

saline water type, with Cl^- and $Na^+ + K^+$ as anions and cations, respectively. They show high geochemical temperatures (T_{sio_2} from 147 to 229°C, $T_{Na-K-Ca}$ from 193 to 235°C and a shifting of oxygen isotopic ratios from the meteoric line (no. 76–B–3=65, 76–B–26= 72, BA–1 =82, BA–2 = 83). From these data, we can infer a deep-seated origin for these hot spring waters. The very high (around 40 ppm) boron (B) content of Acupan Mine hot spring waters may be derived from the host rocks itself or directly from volcanic gases. On the other hand, the lithium (Li) content (around 5 ppm) of extremely high in comparison with the other samples, suggesting that these waters may be derived directly from the Balatoc plug host rocks, which consist of intermediate volcanic rocks.

Assuming tentatively that hot spring waters with such properties represent hot waters of deep origin, it can be deduced that some of the waters collected from Itogon (76–B–11 = 68) and Antamok (76–B–12 = 69) are also of deep origin.

The other samples from Acupan Mine (no. 32 to 34, 38 to 41, 66, 67) have chemical compositions dominated by sulfate (SO_4^{2-}) and calcium (Ca^{2+}) and isotopic compositions plotting near the meteoric line on the $\delta D - \delta^{18}O$ diagram. They may thus represent hot spring waters derived from surface waters or shallow ground waters. As shown clearly by the distribution map (Fig. II–2–26), hot waters of these type are distributed outside the Balatoc plug all around the area of the saline water of deep origin already described. The process of formation of hot spring waters of Ca^{2+}–SO_4^{2-} type be as follows: Hot water rising along Balatoc plug could, after dissociation of SO_4^{2-}, scatter above and around the plug, mix there with surface waters and dissolve some Ca^{2+} from the rocks. Hot spring waters of this type appear at Antamok (no. 18, 19, 20, 26, 70, 71) and Laboy (no. 80, 81), whereas samples from Itogon (no. 1, 44, 45, 53, 54, 75, 76) and Dalupirip (no. 3 to 5, 74) represent intermediate type waters.

The other samples from Asin, Klondyke and Pugo are assumed to represent non-volcanic of Quaternary, saline waters different from the two types previously described.

On the entire area investigated several hot springs are distributed with contrasting properties but, as shown for example by the relationship between $\delta^{18}O$ value and elevation of sampling point (Fig. II–2–29), these hot springs formed, in a relatively restricted domain of isotopic composition, in mutually independent geothermal convective systems. Only in the case of Acupan and Itogon, the similarities between these two springs suggest that they are related to the same geothermal reservoir. As far as can be judged from the results of the geochemical survey of hot springs of the area, the future geothermal exploration should be restricted to areas where saline type hot waters of probable deep origin are known, i.e. around Acupan Mine and partly around Itogon and Antamok Mine.

CHAPTER 3 GRAVITY SURVEY

CHAPTER 3 GRAVITY SURVEY

3–1 Objective of Gravity Survey

Gravity survey is widely used in the early stage of the geothermal exploration to know the basement geological structure, faults, graben, horst and igneous activity such as latent intrusive rocks based on the difference of the rock density.

Furthermore, gravity surveys are used to confirm the structures interpreted by geological surveys and other means of geophysical explorations.

According to the gravity surveys conducted in the known geothermal fields, most of the hot springs and geothermal power plants are located at or adjacent to large scale gravity lows.

Such large scale gravity lows suggest the presence of grabens and depressions at depths which could be a good reservoir of geothermal fluid.

In this survey, the purpose of gravity survey is to detect the subsided structure which is closely related with geothermal reservoir and fault system which bring geothermal fluid to the surface.

3–2 Method of Survey

3–2–1 Abstract

The earth's gravity is a composite force combining the attraction due to the earth's mass and the centrifugal force caused by the earth's rotation. If the earth were a perfect sphere and its density distribution was spherically symmetrical, the gravity value would be the same anywhere on its surface.

Centrifugal force is maximum on the equator and zero on both poles, and direction of action is always opposite that of gravity.

Therefore, gravity becomes maximum on the poles and minimum on the equator. The difference between the maximum and the minimum gravity values is 0.3% which is almost negligible.

A body on the surface of the earth has a "weight" which results from the gravitational attraction between the body and the entire earth. If the body is allowed to fall, it is accelerated by this weight. The unit of acceleration is the gal, named after Galileo and 1 gal is 1 cm/sec^2. The average acceleration on the earth's surface is about 980 cm/sec^2=980 gals (increases by about 0.3% from equator to pole).

Gravitational anomalies are only very small fractions of the earth's field, so a smaller unit is needed. The unit commonly used in gravity survey is the milligal or mgal which is 0.001 gal.

Anomalies from local geologic structures are commonly in the order of one to ten mgals.

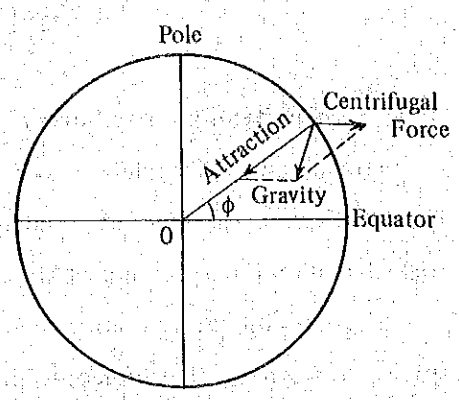

3–2–2 Survey Planning

A total of 303 observation (gravity) stations were planned by the JICA survey team as shown in the location map (Fig. II–3–1). However, actual observed gravity stations were 310. Among these, the altitude of 298 stations were measured by leveling while the remaining 12 stations were measured by a microbarometric altimeter.

The numbering of the stations were from 1 to 309 except for gravity base station which is numbered No.900. The gravity survey was carried out over 220 km^2 area with stations approximately spaced at 500 m. Location of the points were connected by transit and partly by a pocket compass to augment survey accuracy.

Gravity stations were planned and located based on an older (1961) topographic map, hence actual locations of several proposed stations were reestablished in the field.

3–2–3 Gravity Meter

A La Coste D type gravimeter was used. Below are the instruments specifications and functions.

Type and Serial No.	:	D-75
Operating Range	:	200 mgal
Accuracy	:	0.002 mgal
Drift Rate	:	1 mgal/month
Repeatability	:	0.005 mgal
Temperature of Heater	:	52.3°C
Date of Production	:	February, 1982
Dimension	:	197 x 178 x 251 (mm)
Meter Weight	:	3.2 kg
Net Weight	:	10 kg
Gravimeter Constant	:	1.3701
Reading line	:	3.10

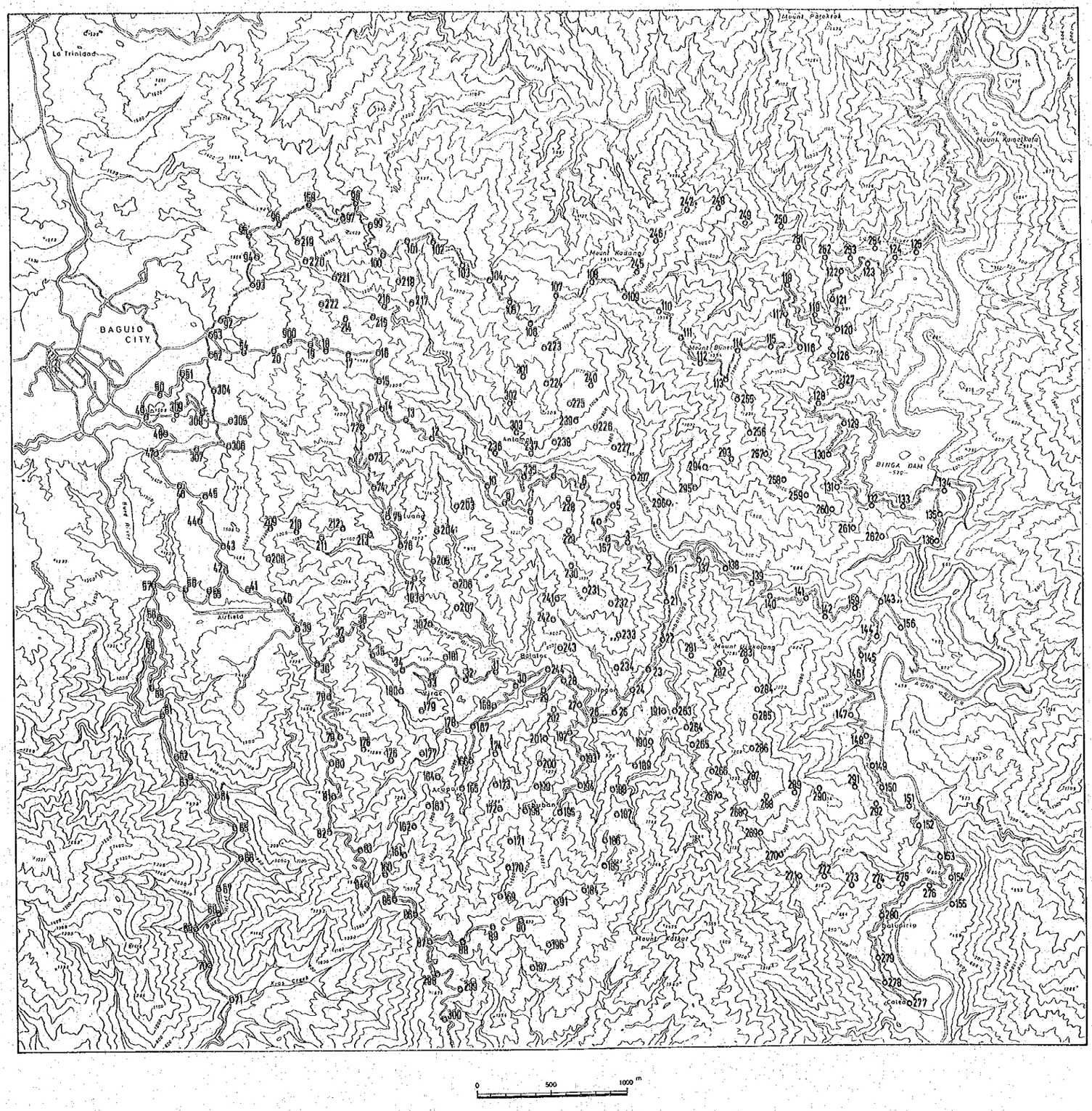

Fig. Ⅱ-3-1 Location Map of Gravity Station

3–2–4 Comparison of Standard Gravity

The known standard gravity station in Baguio City was not located, hence gravity comparison was just made between the gravity station in Muntinlupa, Metro Manila and base station No. 900.

The value at Muntinlupa belonging to the Potsdam system was adapted in the survey considering future connections with gravity network in the Philippines.

Comparison of gravity value at No. 900 with that of Muntinlupa is shown on Table II–3–1.

Table II–3–1 Gravity Standard Value

	Latitude	Longitude	Date	Time	Reading Value	Instrument Height (m)
Muntinlupa	N°14 22.5'	E°121 0.9'	1982.10.1	9h 56m	191.497	0.230
G 900	N°16 25.0'	E°120 37.6'	1982.10.9	7h 53m	71.275	0.275

	Milligal Value	Earth Tide Correction	Instrument Correction	Corrected Value	Gravity Difference	Gravity Value
Muntinlupa	250.995	0.157	0.071	251.223	978,115.247	978,366.470
G 900	93.420	0.042	0.085	93.547	978,115.247	978,208.794

3–2–5 Leveling

(1) Direct Leveling

The direct leveling method was adapted for 298 of 310 points using leveling instruments made by Karl Zeis and Auto Level B-2 of Sokkisha, Japan.

A reference bench mark AGM-1 (16°23.24' N, 120°40.55' E, 801.580m ASL) which belongs to Benguet Corporation was used in this area. Leveling network is shown on Fig. II–3–2, in which leveling of the main route was conducted by JICA surveyor and the secondary route (80 line-km with 131 stations starting from main route) was measured by BED surveyors.

Among the stations on the main routes, 56 stations from No. 1 to 54 along 30 line-km formed a closed loop establishing a closure error of only 213 mm which satisfy the maximum closure error $\in \leqq 100\sqrt{D}$, where D is a line-length in km.

(2) Leveling by Microbarometric Altimeter

Altitude of 12 points were measured by microbarometers made by Negretti and Zambra of UK.

Altitude difference of M-197A of 2 srations were calculated by the following formula by

giving the ratio of pressure at two points.

$$\Delta H = \log \frac{\text{pressure of the station}}{\text{pressure of the known point}} \times 18{,}464$$

$$\times (1 + 0.003665 \times \text{average temperature of two points})$$

As in leveling, a traverse starts from a point of known elevation and closed on the other known elevation. The error of the traverse is time alloted on each reading after making the above mentioned corrections.

3–3 Gravity Correction

Several corrections should be made on the observed gravity value to determine the Bouguer anomaly. Usually, these corrections are divided into two processes which are from the observed gravity value to the absolute gravity value and from the absolute gravity value to the Bouguer anomaly.

3–3–1 Data Processing

The data processing of the gravity value is shown by the following flow chart:

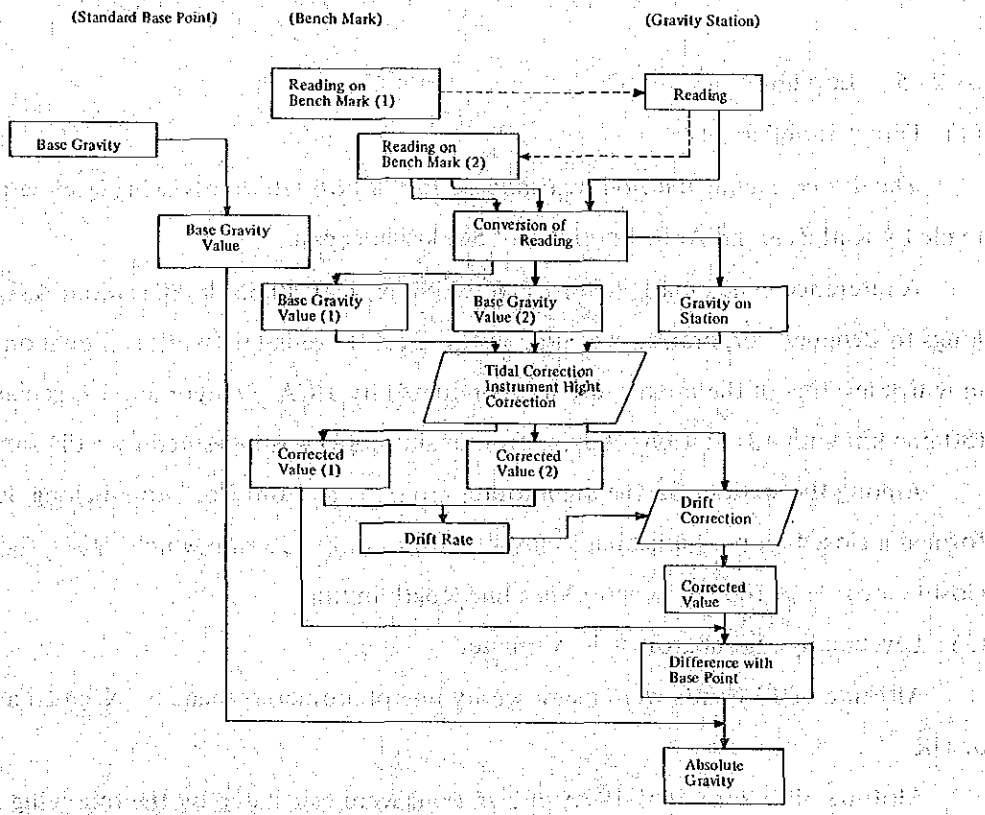

Fig. II–3–3 A Flow Chart of Data Processing of Gravity Data

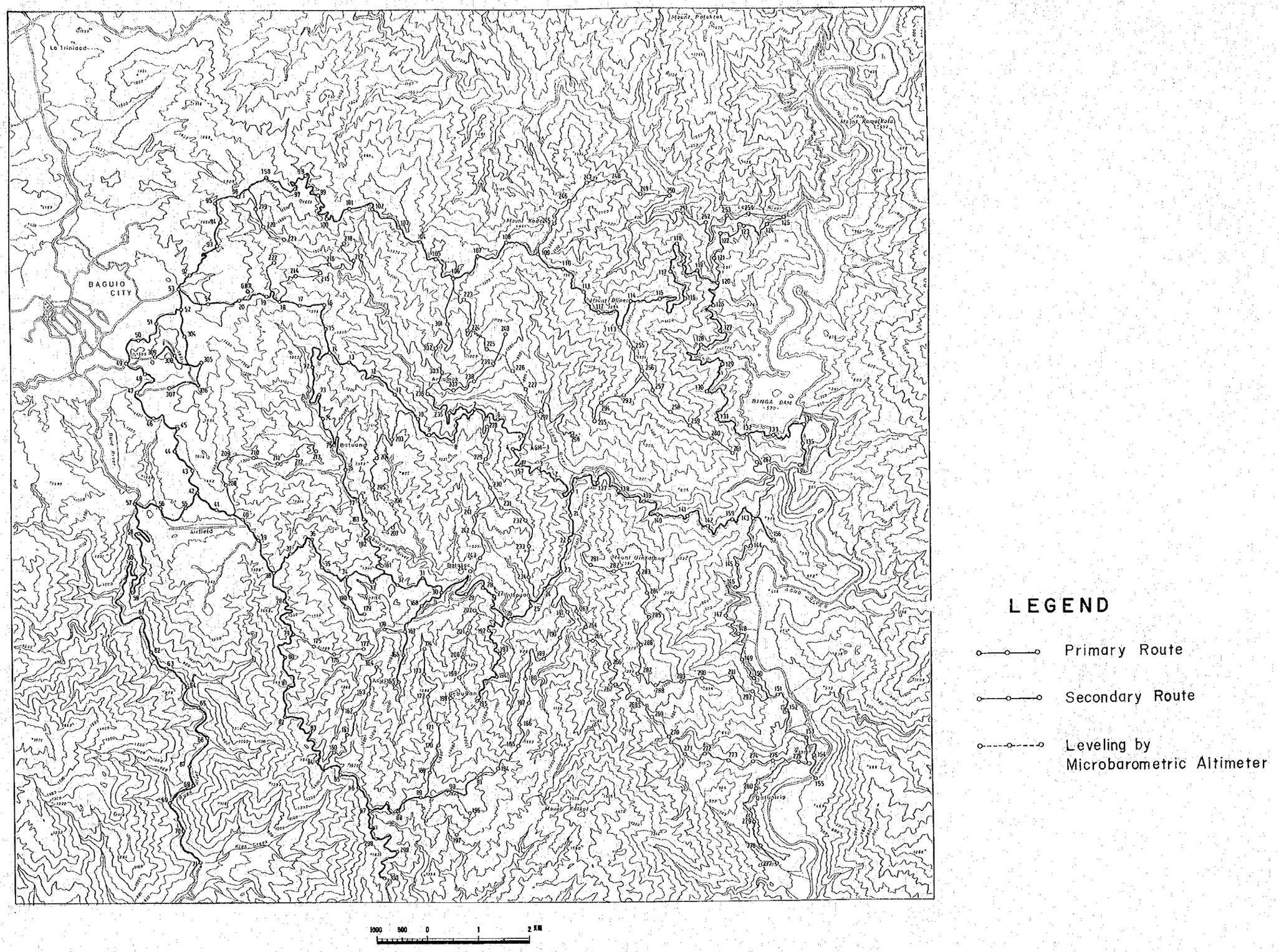

LEGEND

- Primary Route
- Secondary Route
- Leveling by Microbarometric Altimeter

Fig. Ⅱ-3-2 Route Map of Levelimg Surrey.

(1) Conversion

To obtain gravity in milligals from the reading of the counter and dial, the conversion factor (k) is employed. The conversion factor is given for each La Coste gravity meter. The value of gravity milligals is calculated simply multiply the counter reading by the conversion factor. The value of factor for La Coste D75 is 1.3701.

$Vrk = kVr$

Vrk : Observed gravity value in milligals

Vr : Counter reading

k : Conversion factor

(2) Tidal correction

Tidal force is due to the attraction of the sun and the moon at the earth's surface which deviate in direction, and intensity, with time and from place of observation.

Tidal force due to the sun and the moon is calculated by the following formula:

$$Vet = -\Sigma 1.16u$$

$$u = -\frac{3}{2} \cdot G \cdot M \cdot \frac{a}{r^3} \left\{ 3\left(\sin^2 \delta - \frac{1}{3}\right) \cdot \left(\sin^2 \varphi - \frac{1}{3}\right) + \sin 2\delta \cdot \sin 2\varphi \cdot \cos\theta + \cos^2 \delta \cdot \cos^2 \varphi \cdot \cos 2\theta \right\}$$

where,

Vet : Tidal correction

u : Tidal force of the planet

G : Gravitational constant

M : Mass of the planets (the sun and the moon etc.)

a : Distance from center of earth to observation point

r : Distance between earth and planet

δ : Declination of the planet (angle from equator to south or north)

φ : Latitude at observation point

θ : Angle of the planet (angle between terrestrial and planetary meridian plane)

In order to check the tidal corrections, gravity observations on a constant station have been made. Gravity values on the constant station changes together with the changes on tidal forces. The tidal force variations can be confirmed by observing changes for more than 12 hours. Two peaks and a bottom were observed for 14 hours from 0:40 P.M. Nov. 18, 1982 to 2:40 A.M. Nov. 19, 1982 at No. 900.

Good agreement between values was observed for the period with a slight scattering of +0.0721 mgal on the peak and −0.1495 mgal on the bottom. The error is only less than 0.014 mgal.

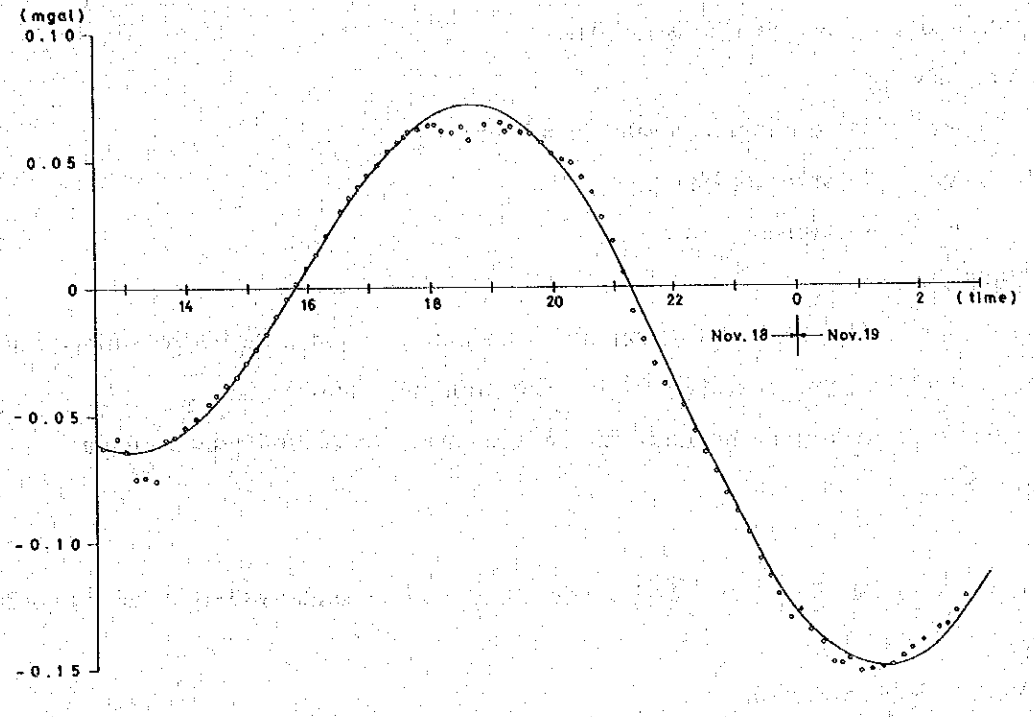

Fig. II–3–4 Diurnal Variation at Gravity Station

(3) Instrument height correction

This correction is used to adjust the instrument height from the station elevation surveyed by leveling.

$Vhi = 0.3086\ hi \times 10^{-2}$

where,

Vhi : Correction of instrument height

hi : Height from station level to top of gravity meter (cm)

(4) Drift correction

Drift is an inherent characteristic error of a gravity meter which changes proportionally with time. The rate of change in drift is not always constant as it depends upon the characteristics of a gravity meter, temperature and pressure of the atmosphere and the way of handling the instrument. Thus, in this survey the closure error was regarded as drift and distributed by time allotment.

(5) Absolute gravity

Corrections on the observed value are as follows:

$$Vc = Vrk + Vet + Vhi + Vd$$

where,

Vc : Corrected gravity value

Vd : Drift correction value

The absolute gravity (g) is observed by adding a difference (Dg) of corrected gravity value (Vc) and the corrected gravity value at the base observation point (Vg) with the absolute gravity value of the base observation point (Bg), which has corresponding value to the International Standard Gravity Value.

$$Dg = Vc - Vg$$

$$g = Bg + Dg$$

3–3–2 Correction of Gravity

A flow chart of various corrections from the absolute gravity to the Bouguer anomaly is shown below.

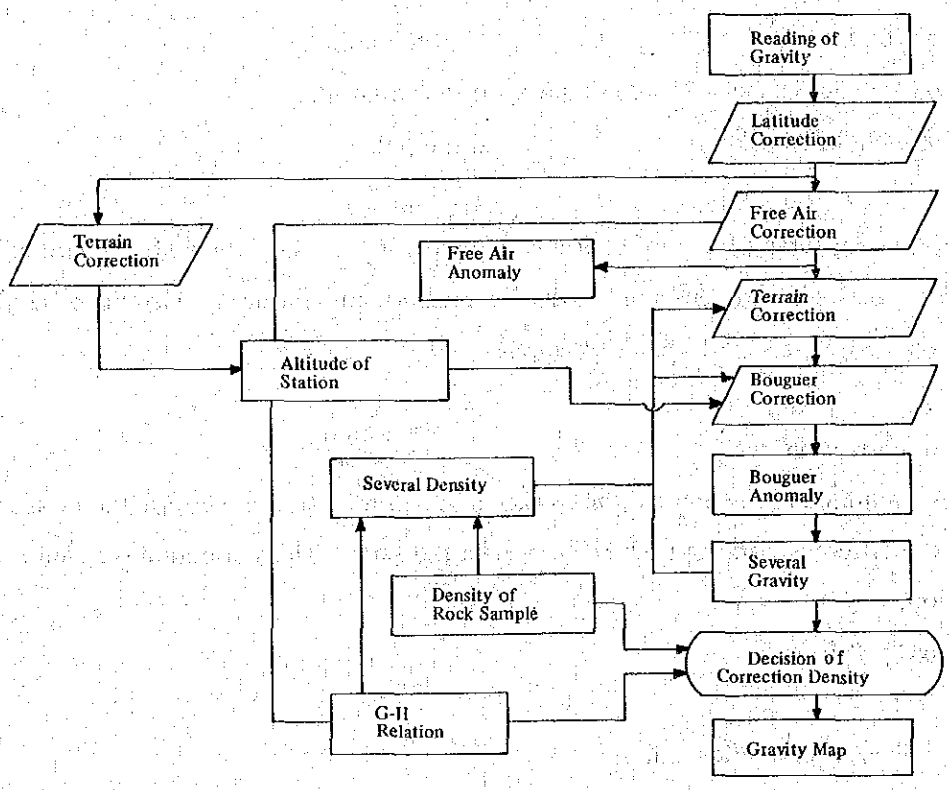

Fig. II–3–5 A Flow Chart of Various Corrections

To compare with observed gravity values at different places, the gravity difference should be based on a base plan. That is, corrections for effect of the centrifugal force, the elevation and the topography. These are called Latitude correction, Free air correction, Bouguer correction and Terrain correction, and the corrected gravity value is called Bouguer anomaly.

(1) Latitude correction

The gravity on the earth decreases towards the equator and increase towards the pole, because of the centrifugal force resulting from the earth's rotation and of the earth's radius due to polar flattening. The correction for this effect is called Latitude correction.

As is the function of latitude ϕ , gravity anomaly which is the difference of absolute gravity and theoretical gravity includes the latitude correction in itself.

In 1930 International Gravity Formula was adopted by IUGG (International Union of Geodesy and Geophysics) which is,

$$\gamma_{1930} = 978.0490\ (1+0.0052884 \sin^2 \phi - 0.0000059 \sin^2 2\phi)$$

but later in 1967 IUGG recommended to use the Normal Gravity Formula, as shown below,

$$\gamma_{1967} = \frac{a\gamma_E \cos^2 \phi + b\gamma_P \sin^2 \phi}{\sqrt{a^2 \cos^2 \phi + b^2 \sin^2 \phi}}$$

$a = 6{,}378{,}140$ m : Radius of the earth at the equator

$b = 6{,}356{,}180$ m : " at the pole

$\gamma_E = 978.032$ gal : Standard gravity at the equator

$\gamma_P = 983.218$ gal : " at the pole

In this gravity survey the above formula is used for the calculation of standard gravity. The difference between International Gravity Formula γI and Normal Gravity Formula γN is,

$$\gamma N - \gamma I = -17.2 + 13.6 \sin^2 \phi \text{ (mgal)}$$

(2) Free air correction

This is a required correction for the elevation of a gravity station because the measurement was made at a different distance from the center of the earth. This correction is called Free air correction.

$$\delta gO = \beta \cdot Hm$$

where,

δgO : Free air correction value

Hm : Altitude of the gravity station (m)

β : The gravity gradient between the gravity station and the sea level (called Free air correction factor, usually 0.3086)

(3) Terrain correction

A topographic irregularity (hill, knoll, slope, etc.) will exert an attraction directly proportional to its desntiy. The vertical component of this attraction will be directed upwards and this reduces the gravity.

A term of this magnitude must therefore be added to the measured value of gravity. A station near a valley is a negative mass and the vertical component of its attraction will also be directed upwards leading again to an additive topographic correction.

The topographic correction is calculated by dividing the area around a station in compartments into 5 groups, namely, "far", "medium", "near", "neighbor", and "close".

The range and size of grid are as follows.

Table II–3–2 Range and Size of Grid for Topographic Corrections

Kinds of Correction	Range radius (km)	Grid Interval X (m) (min)	Grid Interval Y (m) (min)	Topographic Map Used
Far	16.00 – 64.00	7,108 (4')	7,376 (4')	1/200,000
Medium	4.00 – 16.00	1,777 (1')	1,844 (1')	1/ 50,000
Near	1.00 – 4.00	444.3 (0.25')	461.0 (0.25')	1/ 50,000
Neighbor	0.02 – 1.00			1/ 25,000
Close	0.00 – 0.02			sketch

The range of correction listed above means the radius of a circular plate with the gravity station as its center and without overlapping.

(a) Terrain correction of far, medium and near

For the correction of far, medium and near, altitude informations are based on the grid of latitude and longitude of a cartesian co-ordinate and the altitudes are read by a circular plate shown in Fig. II–3–6.

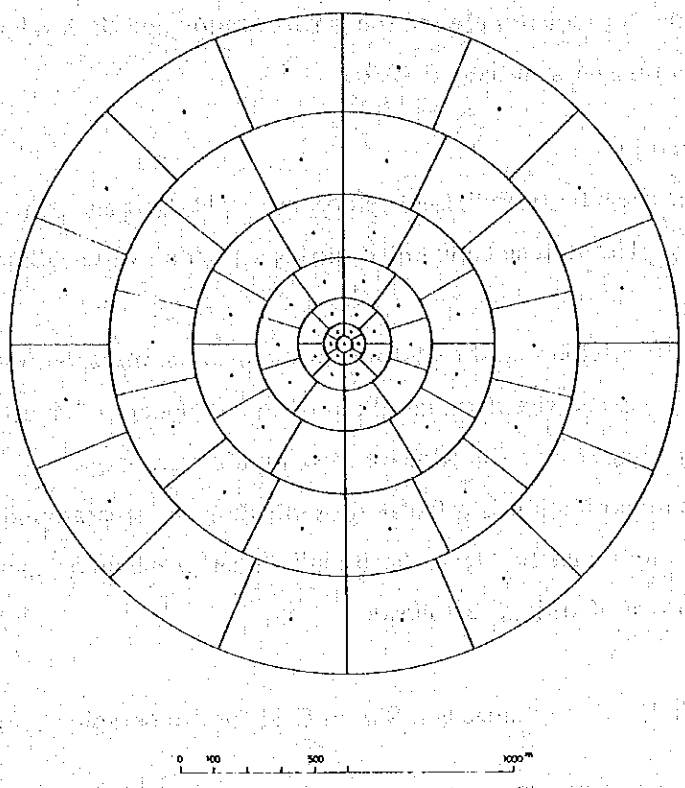

Fig. II–3–6 Disc Used for Topographic Correction (Far, Middle and Near)

Average of all altitudes in each component is used for the correction and total computed terrain correction by a formula shown below is called far, medium or near depending upon the size of the radius.

$$\delta_{go'} = \frac{2\pi}{n} G\rho \left(R_1 - R_2 - \sqrt{R_1^2 + (H - H')^2} + \sqrt{R_2^2 + (H - H')^2} \right)$$

where,

$\delta go'$	:	Terrain correction
n	:	Number of component
G	:	Gravitaional constant
ρ	:	Correction density
R_1	:	Shorter radius of a component
R_2	:	Longer radius of a component
$H - H'$	:	Difference of altitude between station and average height of a component

A component in the circular plate is designed to involve at least one grid intersection of latitude and longitude.

(b) Terrain correction of neighbor

For the correction of neighbor a circular plate divided into 66 components as shown in Fig. II–3–7 with radius of 20 to 1000 m is used. The same method and formula are adopted for the calculation.

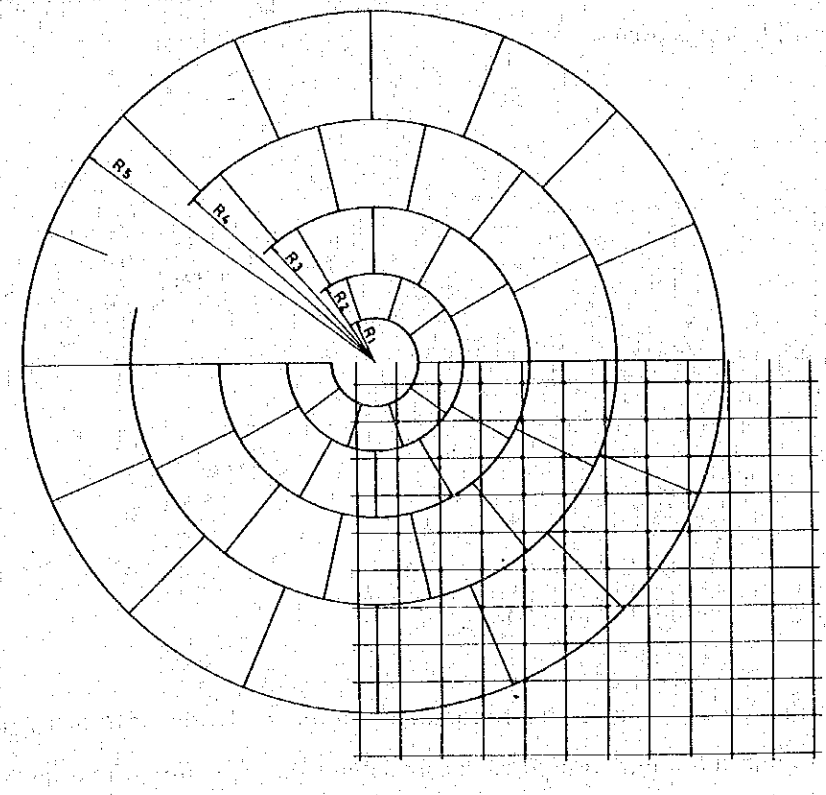

Fig. II–3–7 Disc Used for Topographic Correction (Neighbor)

(c) Terrain correction of close

The nearest topography within 20 m from the gravimeter is sketched and a two-dimensional topographic section is simply modified as mentioned below. The correction due to the close cliff, slope and channel are calculated as,

$$\delta go' = G\rho \int_D^R \int_{-\sqrt{R^2-X^2}}^{\sqrt{R^2-X^2}} \int_0^{H+(X-D)\tan\beta} \frac{Z\, dXdYdZ}{(X^2+Y^2+Z^2)^{3/2}}$$

$$= 2G\rho\int_D^R \int_{-\sqrt{R^2-X^2}}^{\sqrt{R^2-X^2}} \left(\frac{1}{\sqrt{X^2+Y^2}} - \frac{1}{\sqrt{X^2+Y^2+(H-D\tan\beta)^2}} \right) dXdY$$

$$= 2G\rho\int_D^R \left(\log \left| \frac{R-\sqrt{R^2-X^2}}{R+\sqrt{R^2-X^2}} \right| - \log \left| \frac{\sqrt{R^2+(H-D\tan\beta+X\tan\beta)^2}-\sqrt{R^2-X^2}}{\sqrt{R^2+(H-D\tan\beta+X\tan\beta)^2}+\sqrt{R^2-X^2}} \right| \right) dX$$

This integration can not be expressed by a primary function, then a digital integration by means of Simpson 1/3 law is used.

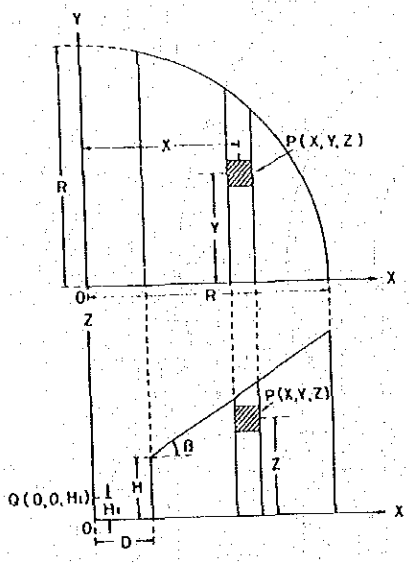

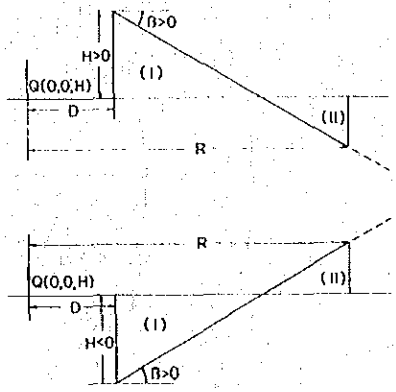

When the terrain is rugged, the topography should be divided into many blocks as shown below and the summation of each calculated values becomes the total correction of close.

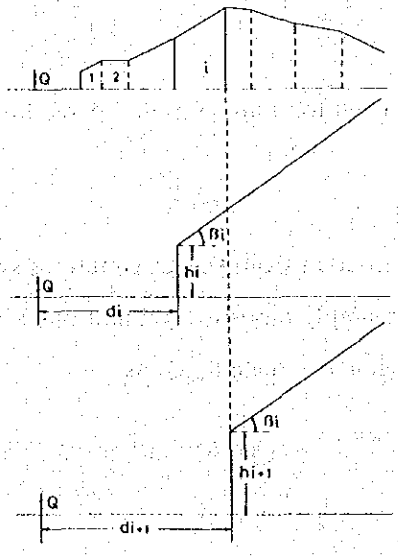

(4) Bouguer correction

Bouguer correction is one of the height correction caused by the presence of the rock mass between the station and the sea level. Bouguer correction is given as follows.

$\delta go'' = -2\pi G\rho Hm = -0.0419\rho Hm$

ρ : Specific gravity (density) of the intervening rock

3–3–3 Bouguer Anomaly

Bouguer anomaly is given as follows,

$\Delta g_O = g - \gamma + \delta g_O + \Sigma go' + \delta go''$

where,

Δg_O : Bouguer anomaly value

The Bouguer anomaly value varies on the density for Bouguer correction and Terrain correction. In this gravity survey, the density for correction is assumed by these method as mentioned below and by their combination.

(1) Density of rock samples

In this survey, 186 rock samples were collected on the ground surface by the geological team and measured their densities. Table II–3–3 shows the average and distribution of density

Table II–3–3 Average Density and Distribution of Rock Samples

Period	Formation	Rock (Number of Sample)		Average		Density 2.2 2.4 2.6 2.8 3.0
Quaternary	Terrace Dep.	Gravel		Unmeasured		
	Balatoc Plug	Dacitic Pyroclastic Rock (9)		2.47		
Tertiary	Klondyke	Conglomerate, Pyroclastic R., Tuff, Sand S. & Mud S. (26)		2.58	2.68	
	Zigzag	Andestic Pyroclastic Rock (3)		2.72		
	Pugo	Metavolcanic Rock & Metasedimentary Rock (23)		2.78		
Upper Cretaceous	Dalupirip	Schist (14)		2.83		
Intrusive Rock	Andesite Porphyry (12)			2.69		
	Intermediate Volcanic - Plutonic Complex	Northern Part (12)		2.74	2.70	
		Southern Part (10)		2.65		
	Pyroxene Andesite Porphyry (8)			2.73		
	Acidic to Intermediate Volcanic - Plutonic Complex (4)			2.68		
	Granodiorite (8)			2.82		
	Gabbroic Diorite (3)			2.76		
	Quartz Diorite	Southern Part (30)		2.66	2.71	
		Northern Part (21)		2.79		

of the rock samples that were measured. The average densities vary from 2.47 to 2.83. But this is considered to vary from 2.58 to 2.83 without Balatoc Plug which is an intrusive rock and is distributed in a narrow and limited area. In this survey area, density structure is composed of various rocks that have similar distribution of density. Their average density of all measured rock samples is 2.70. This value should be considered to reduce to a few percentage because of rock alteration and weathering.

(2) G-H Correction

Gravity decreases with the increase of the altitude when the gravity data are plotted as the altitude on lateral axis and latitude corrected gravity on the vertical axis, the gravity data may be scattered near linear line which is,

$$g - \gamma = \Delta go - (\beta - 2\pi G\rho)\,Hm$$

The rate of decrement is nearly equal to the coeffecient of the height correction, $\beta - 2\pi G\rho$. Therefore, the inclination of the linear line fit to the plots represent the average of rock density in the area. Fig. II–3–8 shows the G-H correlation for this gravity survey and the calculated density is 2.86 by least square method (when β is equal to 0.3086).

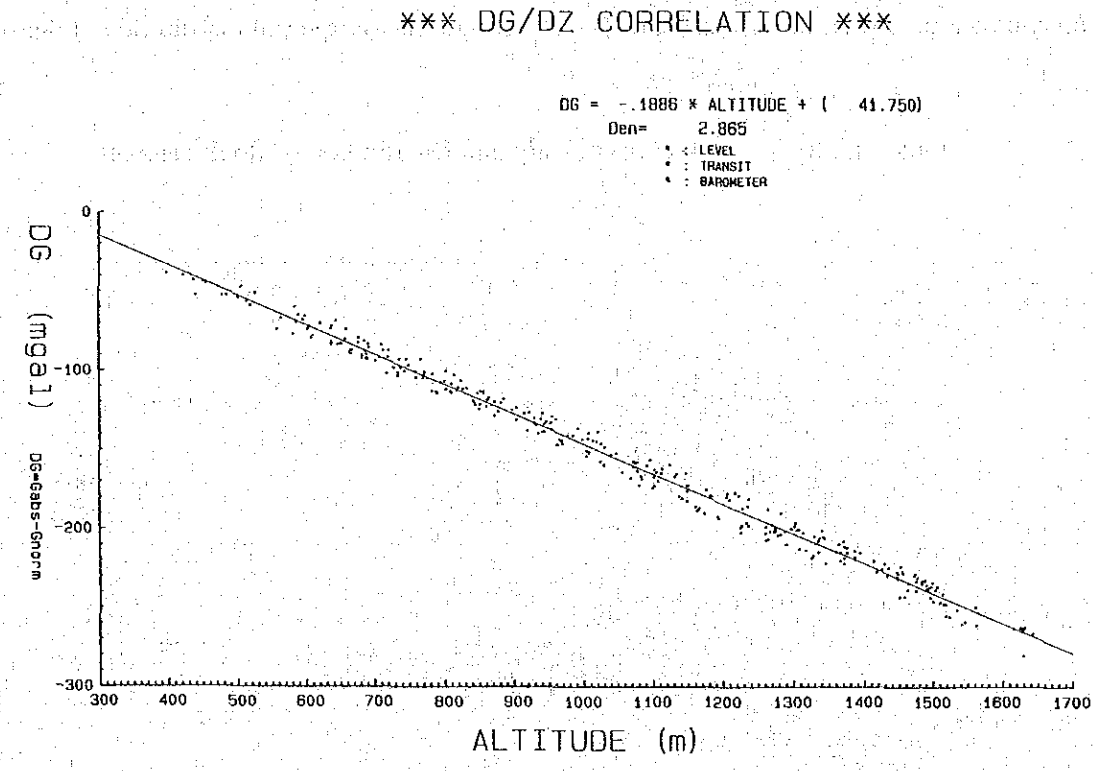

Fig. II–3–8 G–H Correlation Map

(3) Correlation Method

In the Bouguer anomaly map, when the Bouguer anomaly is higher in the mountains and is lower in the valleys, the density of corrections is lower. In the opposit case, the density is higher.

Bouguer anomaly maps are made by several kinds of densities, and are not correlated good with topographical changes which are selected by the above mentioned characteristic.

In this survey, among the assumed density of 2.4 to 2.8, five kinds of densities are used to make Bouguer anomaly maps. Assumed density of 2.6 is selected as it reflects the geological structure better than the others with less terrain effects. On Figs. II–3–9, II–3–10 and II–3–11 Bouguer anomaly maps are shown with the density of 2.5, 2.6 and 2.7, respectively.

3–4 Method of Analysis

Bouguer anomaly measured on the surface is made up of various anomalies for geological structures which have different depth, shape and density. Bouguer anomaly is divided into several "band" by filtering and residual gravity for each band are used for structural analysis corresponding with each wave length. In this survey, high cut filter made use of Fourier transform is enforced.

3–4–1 Residual Gravity

For the purpose of selective detection of gravity anomaly of a certain scale, residual gravity is divided from Bouguer anomaly by means of two kind of high cut filters.

When the gravity potential converted into complex Fourier transform is F (u, v) and number of grid in x and y direction are m and n respectively, this transform is expressed as follows,

$$F(u, v) = \sum_{m} \sum_{n} (G(x, y) \cdot \exp(-i(ux+vy)) \Delta x \Delta y$$

$$G(x, y) = \sum_{m} \sum_{n} F(u, v) \cdot \exp(i(ux+vy)) \Delta u \Delta v$$

If the relation between the above equations is expressed as G (x, y), F (u, v), high cut filter is obtained as,

$$G(x, y) = F(u, v) \cdot \exp(-\lambda(u^2+v^2))$$

where, λ is a parameter corresponding with a wave length of high cut filter, and in this processing, four kinds of residual gravity are obtained with the parameter of $\lambda = 0.25, 2.1, 10.2$ such as $\lambda_{0\cdot25} = (G - G_{0\cdot25})$, $\lambda_{0\cdot25\sim2\cdot1} = (G_{0\cdot25} - G_{2\cdot1})$, $\lambda_{2\cdot1\sim10\cdot2} = (G_{2\cdot1} - G_{10\cdot2})$ and $\lambda_{10\cdot2} = (G_{10\cdot2})$. The latter three are indicated in Fig II–3–12, II–3–13 and II–3–14.

3–4–2 Second Derivative Method

When the second derivative of the gravity anomaly is Gv(x,y), this is expressed as follows,

$$Gv(x,y) = -F(u,v)(u^2 + v^2)$$

Second derivative method has been utilized because it reflects shape of rocks, faults and the other geological structures. In this survey, second derivative method is enforced to detect shape of intrusive rock because many intrusive rocks are distributed in this area. Second derivative map is shown on Fig. II–3–15.

3–5 Results of Analysis

3–5–1 Bouguer Anomaly Map

As discussed in Section 3–4, Bouguer anomaly map with assumed density of 2.6 is the most appropriate for interpretation for this particular area – Acupan Geothermal area.

From Fig. II–3–10 (Bouguer Anomaly Map), Bouger values range from 49 to 77 mgal with contours trending N–S. The central portion of the map featured gravity lows sorrounded by gravity highs. Anomaly (gravity lows) seems to extend towards north and northwest.

Steep gradient change suggesting fault structures is not distinct. Gravity lows could be due to low density Itogon quartz diorite which has a value around 2.66.

Gravity lows observed east of the Acupan Mine could be attributed to the adjacent Balatoc plug (density : 2.47).

Several low gravity zones extending from Itogon to Baguio Airport and from Lucbuban to Kias Creek were believed to be influenced by weakly fractured rocks.

Gravity highs detected northwest of the area, and not so eminent gravity highs outlined around Antamok and Batuang vicinities, correspond to high density intrusive rocks found on both localities.

Another gravity high observed southwest of the area could be correlated to andesite flows and zigzag formation which have a density of 2.72.

High gravity zones in northeastern part of the area conform with the distribution of Itogon quartz diorite. However, density of collected rock samples showed higher density of 2.79.

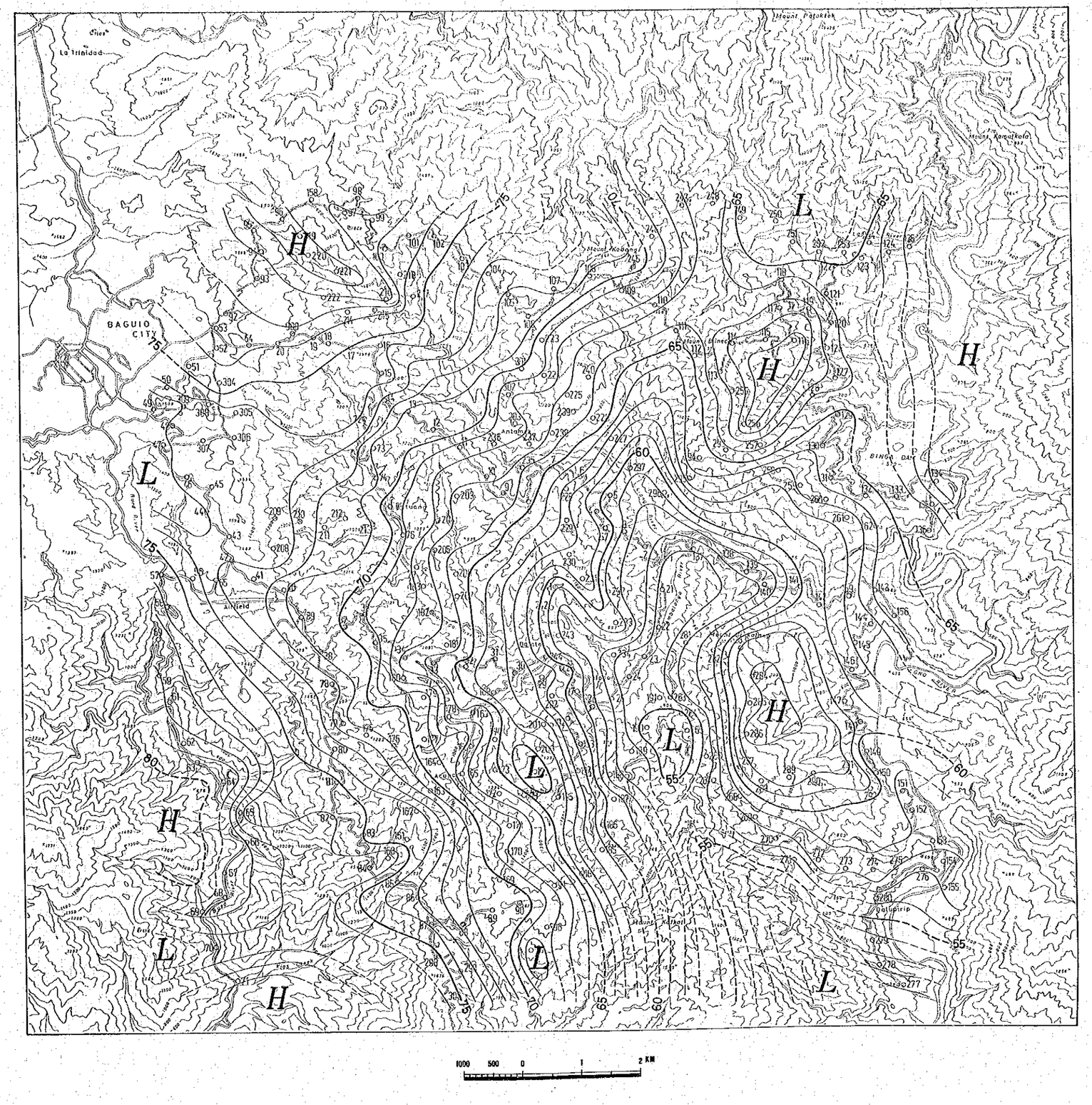

Fig. Ⅱ-3-9 Bouguer Anomaly Map(ρ=2.5)

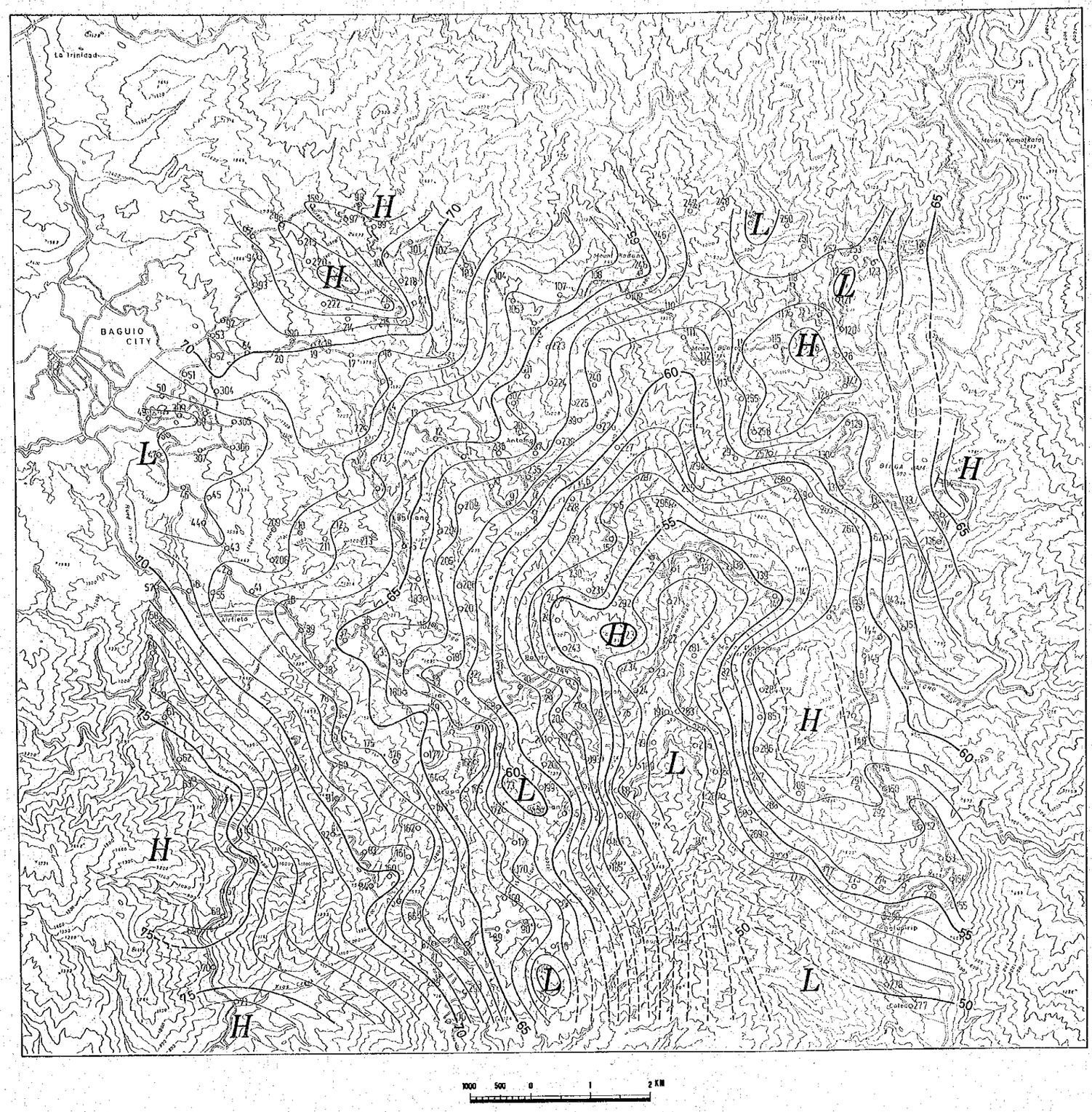

Fig. Ⅱ-3-10 Bouguer Anomaly Map(ρ=2.6)

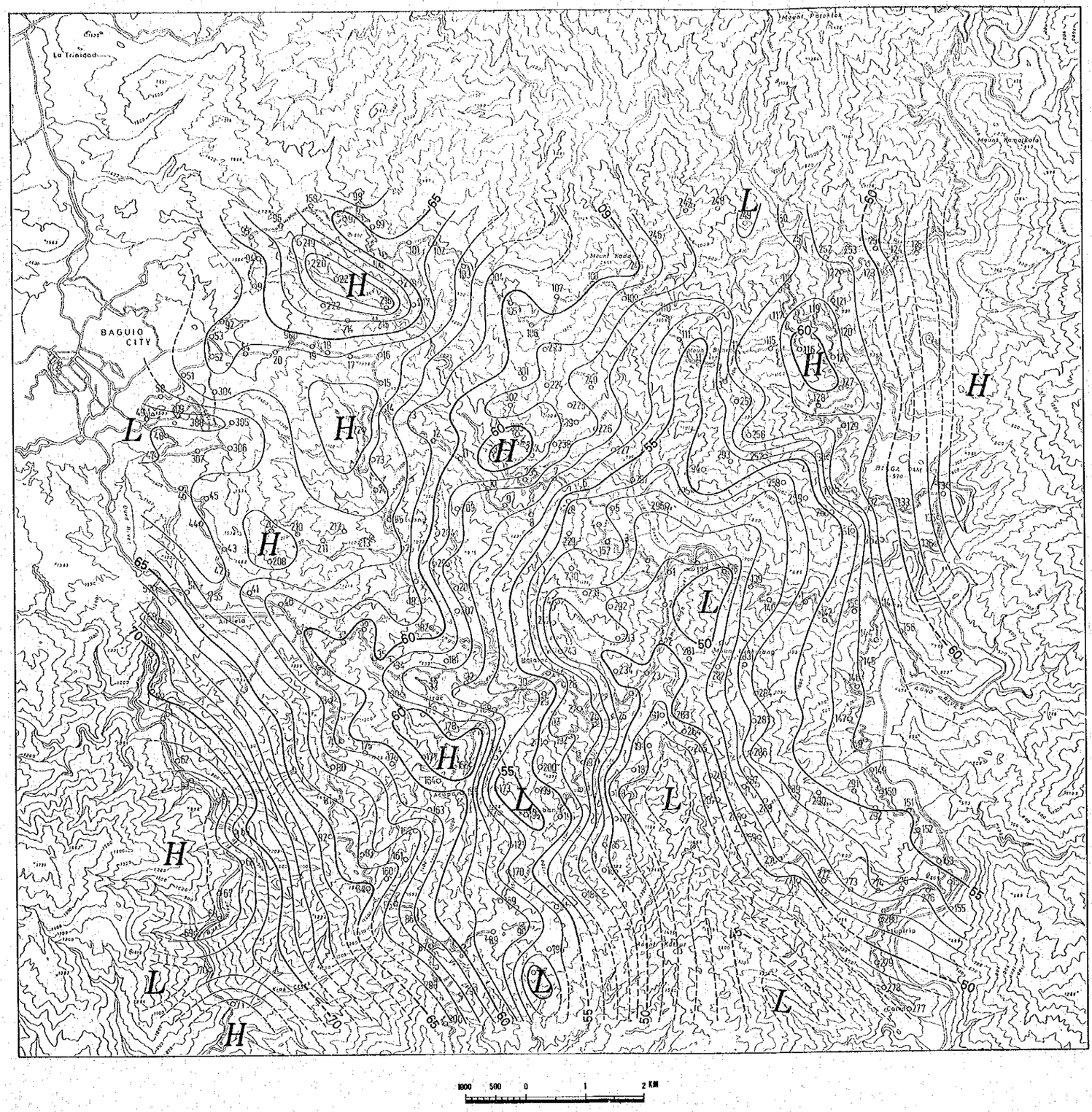

Fig. Ⅱ-3-11 Bouguer Anomaly Map(ρ=2.7)

Fig. Ⅱ-3-12 Residual Map(λ=0.25～2.1)

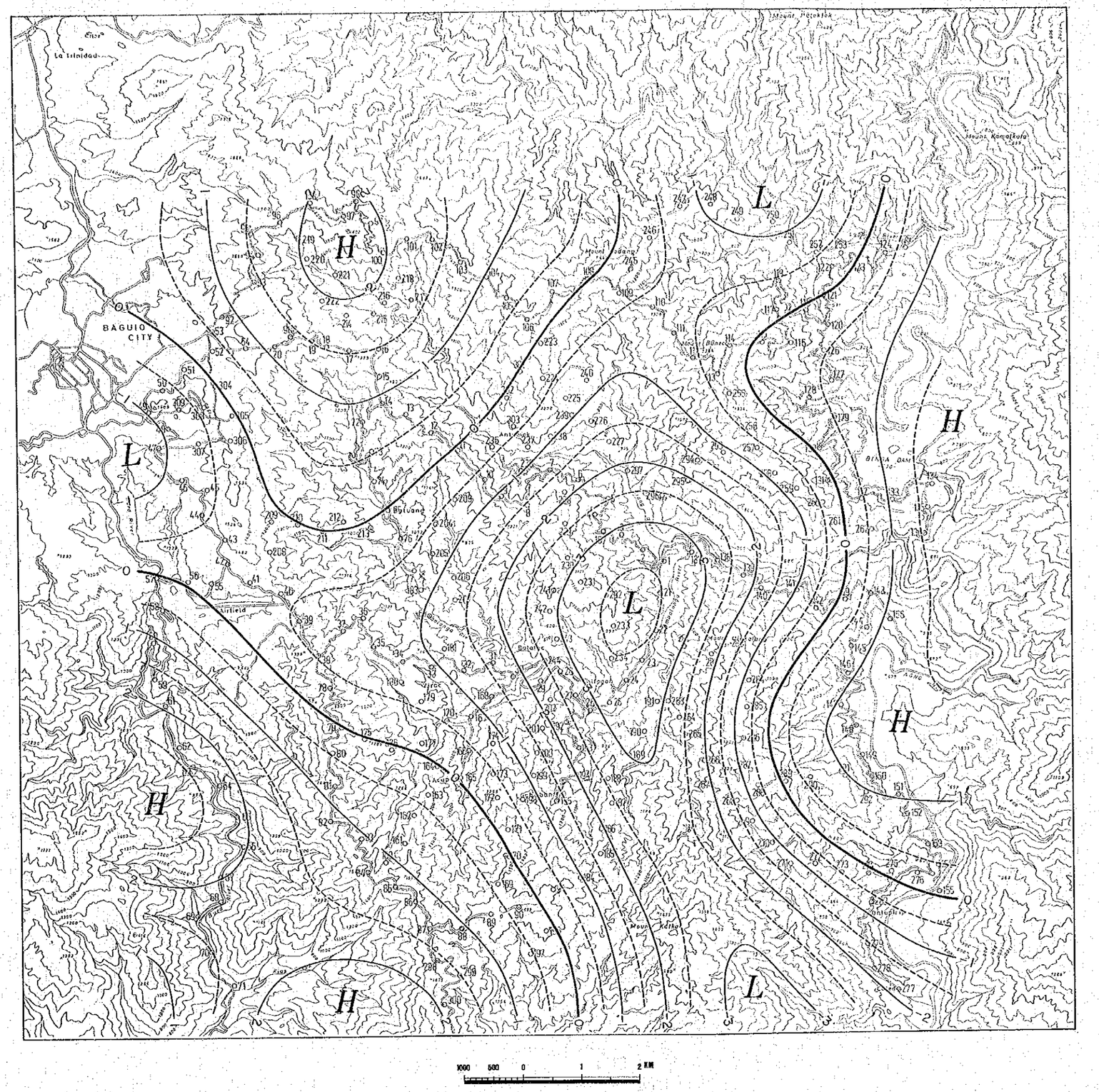

Fig. Ⅱ-3-13 Residual Map(λ=2.1～10.2)

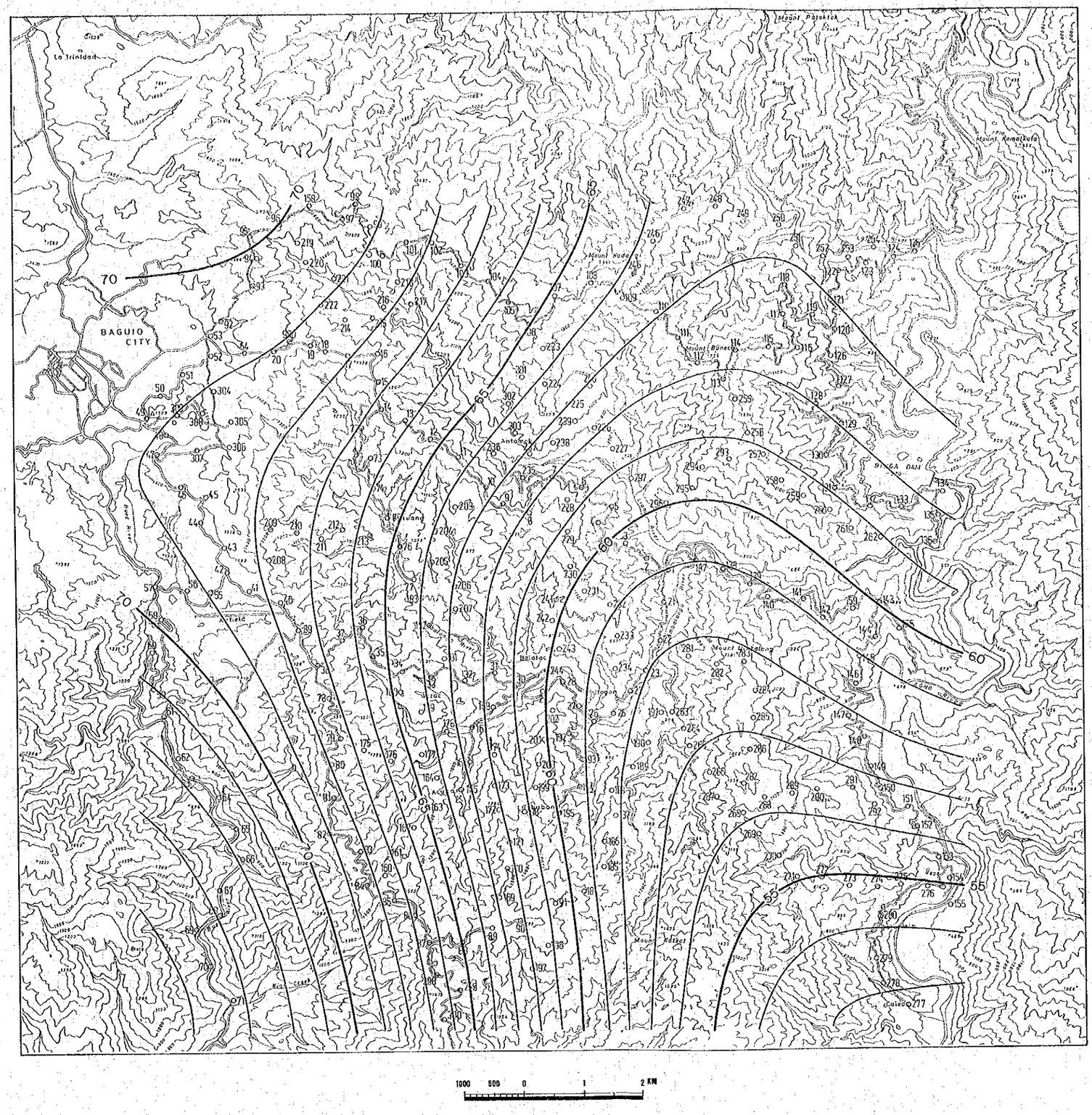

Fig. Ⅱ-3-14 Regional Map($\lambda \geq 10.2$)

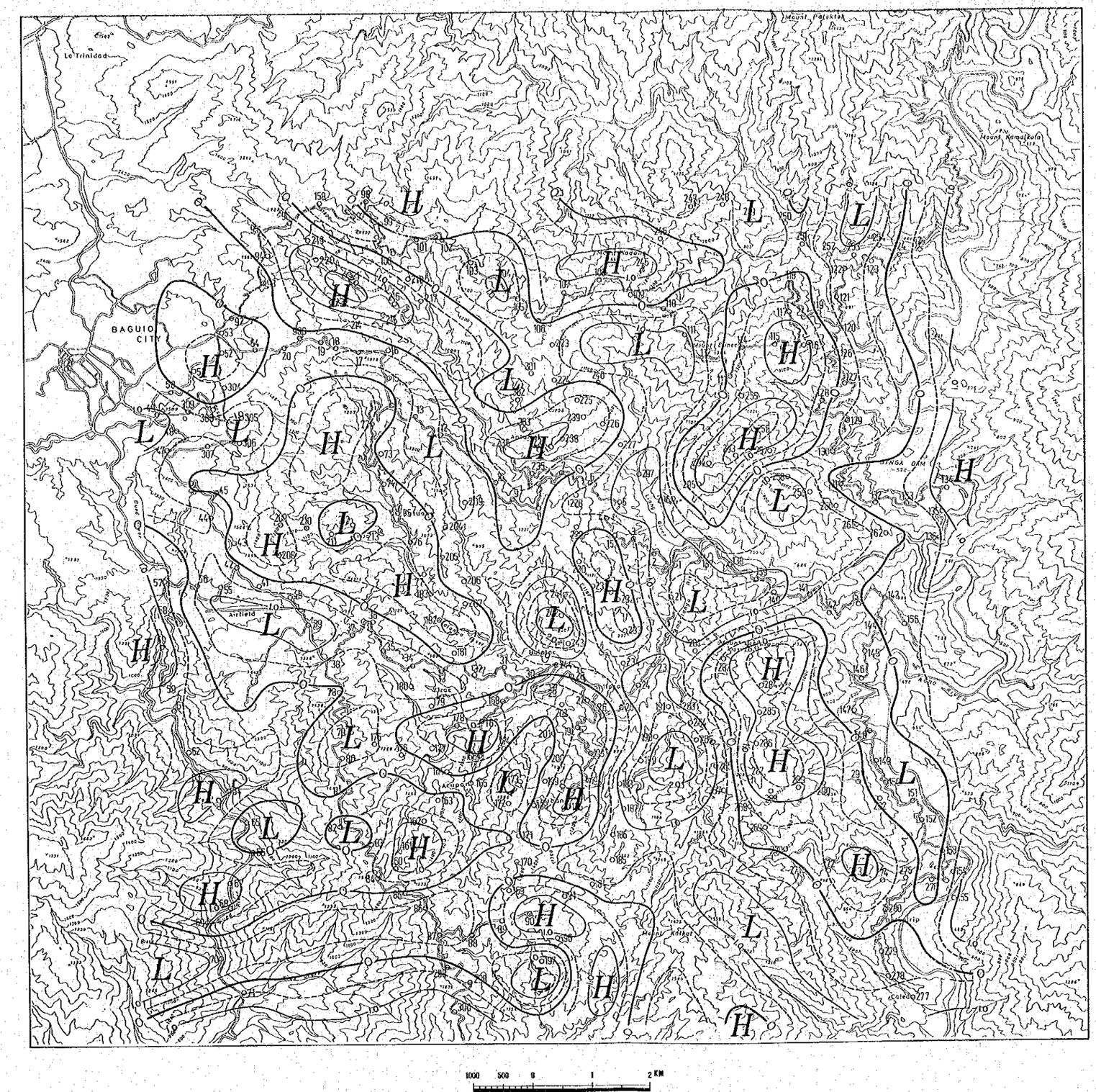

Fig. Ⅱ-3-15 Second Derivative Map